PCCP

Accepted Manuscript

This article can be cited before page numbers have been issued, to do this please use: A. G. Santos, J. T. Marquês, A. C. Carreira, I. R. Castro, A. S. Viana, M. Mingeot-Leclercq, R. F. M. de Almeida and L. C. Silva, *Phys. Chem. Chem. Phys.*, 2017, DOI: 10.1039/C7CP05353C.

View Article Online
DOI: 10.1039/C7CP05353C

Phys. Chem. Chem. Phys.

ARTICLE

The molecular mechanism of Nystatin action is dependent on membrane biophysical properties and lipid composition †

Received 00th June 2017,
Accepted 00th Month 2017

DOI: 10.1039/x0xx00000x

www.rsc.org/

A. G. dos Santos[a,b,c], J. T. Marquês[c], A. C. Carreira [a,c], I. R. Castro[a], A. S. Viana[c], M.-P. Mingeot-Leclercq[b], R. F. M. de Almeida[c,§,*] and L. C. Silva[a,d,§,*]

Nystatin (Nys) is a pore forming broad-spectrum and efficient antifungal drug with significant toxicity in mammalian organisms. In order to develop a non-toxic and more effective Nys formulation, its molecular mechanism of action at the cell membranes needs to be better understod. It is widely accepted that Nys activity and toxicity depends on the presence and type of membrane sterols. Taking advantage of multiple biophysical methodologies, we now show that the formation and stabilization of Nys aqueous pores, which are associated with Nys cytotoxicity, occurs in the absence of membrane sterols. Our results suggest that Nys mechanism of action is driven by the presence of highly ordered membrane domains capable of stabilizing the Nys oligomers. Moreover, Nys pore formation is accompained by strong Nys-induced membrane reorganization that depends on membrane lipid composition and seems to underlie Nys cytotoxic effect. Accordingly, in membranes enriched in a gel-phase forming phospholipid, Nys incorporates within the phospholipid-enriched gel domains, where it forms pores able to expand gel domains. In contrast, in membranes enriched in gel domain forming sphingolipids, Nys-induced pore formation occurs through the destabilization of the gel phase. These results show that Nys mechanism of action is complex and not only dependent on membrane sterols, and provide further insight into the molecular details governing Nys activity and toxicity.

Introduction

Opportunistic fungal infections show high dissemination and proliferation rates in immunodepressed patients, as well as resistance to most common antimicrobial drugs. In fact, fungal resistance to antimycotics has been recognized by the World Health Organization as an emerging health problem [1]. Consequently, the implementation of new antifungal drugs with improved efficacy and lowered adverse effects is becoming increasingly relevant [2].

Polyene macrolide antifungals present a very low antibacterial activity [3] coupled with a potent broad-spectrum antifungal action, proving to be one of the most effective antifungal drug class synthesized by bacteria, in this case *Streptomyces* spp [2]. Amphotericin B (AmB) and Nystatin (Nys) are two important members of this family. Despite its side effects and growing resistance to treatment, AmB is widely used to treat systemic fungal infections. Nys, which presents a higher antifungal activity, is restricted to topical or oral infections[4] due to the lack of a formulation suitable for systemic use. The use of Nys as a viable pharmaceutical alternative to AmB-resistant infections hinges upon the development of an optimized drug carrier. An enhanced understanding of the mode of action of this polyene antifungal at the molecular level will certainly guide the design of alternative strategies to improve drug efficacy and reduce its toxicity.

Polyene macrolides such as AmB and Nys (Scheme 1) are amphipathic molecules, structurally characterized by a large lactone ring with multiple double bounds [3], targeting the membrane of sensitive organisms. Once in the membrane they can form small diameter channels (~ 0.6 nm [5]) that ultimately lead to cell death [3,6]. Typically, sensitive cells, namely fungal and mammalian cells possess sterols - ergosterol (Erg) and cholesterol (Chol), respectively - while resistant cells, bacteria, do not [7]. Accordingly, it has been proposed that Nys and AmB activity/selectivity are linked to either the presence or type of sterols [8]. The most widely accepted model for Nys mechanism of action considers the formation of stoichiometric antifungal-sterol complexes organized as barrel-like membrane-spanning channels [9–11]. The selective toxicity of the polyene antifungal

[a] iMed.ULisboa - Research Institute for Medicines Faculdade de Farmácia, Universidade de Lisboa, Av. Prof. Gama Pinto, 1649-003 Lisboa, Portugal.
[b] FACM/LDRI-UCL - Cellular and Molecular Pharmacology unit of the Louvain Drug Research Institute, Université catholique de Louvain, Avenue E. Mounier 73, B-1200 Bruxelles, Belgium.
[c] CQB - Centre for Chemistry and Biochemistry, Faculdade de Ciências, Universidade de Lisboa, Campo Grande, 1749-016 Lisboa, Portugal.
[d] Centro de Química-Física Molecular and Institute of Nanoscience and Nanotechnology, Instituto Superior Técnico, Universidade de Lisboa, Av. Rovisco Pais, 1049-001 Lisboa, Portugal.
[§] Co-senior authors
[*] Corresponding authors: Liana C. Silva, iMed.ULisboa, Faculdade de Farmácia Universidade de Lisboa, Av. Prof. Gama Pinto, 1649-003 Lisboa, Portugal. Tel: + 351 217 946 429, email: lianacsilva@ff.ulisboa.pt; Rodrigo F.M. de Almeida, CQB - Centre for Chemistry and Biochemistry, Faculdade de Ciências, Universidade de Lisboa, Campo Grande, 1749-016 Lisboa, Portugal, email: rfalmeida@ciencias.ulisboa.pt

† Electronic supplementary information (ESI) available: 3 supplementary figures with supplementary information. See DOI:XXX

View Article Online
DOI: 10.1039/C7CP05353C

between pathogenic eukaryotic organisms and animal cells would then be related to a stronger affinity towards Erg, present

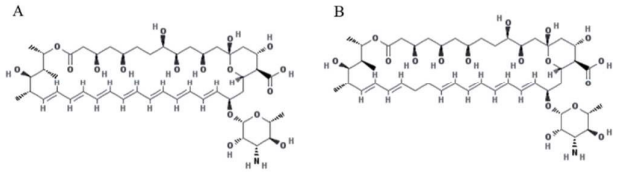

Scheme 1: Chemical structure of **(*A*)** Amphotericin B and **(*B*)** Nystatin drawn using PubChem Sketcher V2.4 from Canonic SMILES.

in the fungal membranes, relatively to Chol found in the membranes of mammalian cells [3].

Despite the general consensus on polyene macrolide mode of action, controversy still persists regarding the role[12] and even the indispensability [13–15] of sterols in Nys self-assembly process that occurs within lipid bilayers. It has been proposed that sterols only assist in the packing of the antifungal molecules by rigidifying the membrane, instead of directly participating in channel formation [16,17]. Other authors have questioned if the presence of a sterol in the membrane is required at all for the polyene antifungals ability to induce membrane leakage [15,18].

The formation of active antifungal species would be facilitated by the presence of an ordered state in the lipid bilayer, whether by incorporation of an ordering sterol in the membrane (such as Erg and Chol)[12,19–21] or of a lipid with a high gel/fluid transition temperature (T_m), which would be in a gel phase at body temperature [22].

Recently, a study carried out in the budding yeast *Saccharomyces cerevisiae,* a Nys sensitive organism, showed a significant fraction of highly ordered sphingolipid (SL)-enriched sterol-free gel-like microdomains in the yeast plasma membrane under physiological conditions [23]. The evidence of gel domains in the plasma membrane of a sensitive organism raises the hypothesis that polyene macrolides may act through a sterol-independent mechanism. This hypothesis is supported by the decreased sensitivity to Nys of certain yeast mutant cells with an altered SL profile and normal levels of Erg [24], and also by recent evidence suggesting the formation of gel-like phases in animal cells [25], such as ceramide-enriched domains in human embryonic kidney cells [26] and SL-enriched domains in human fibroblasts [27], which could explain Nys toxicity.

In this work, we aim to further explore this hypothesis by studying Nys interaction with sterol-free membranes containing gel-phase forming lipids. To this end, two different high T_m lipids, the SL egg sphingomyelin (ESM) and the glycerophospholipid 1,2-dipalmitoyl-*sn*-glycero-3-phosphocholine (DPPC), were mixed in varying proportions with a fluid phosphatidylcholine. With this strategy, it was possible to analyze and distinguish the effects of the presence of a gel phase, membrane physical properties and lipid composition on Nys-membrane interactions and mechanism of action. Taking advantage of Nys intrinsic fluorescence and using atomic force microscopy (AFM), we showed that the presence of a gel phase enhances Nys partition into the membrane and that, in the absence of sterol, Nys-bilayer interaction is dependent on membrane lipid composition and biophysical properties, which dictate subsequent Nys and lipid organization, as well as Nys action.

Materials and Methods

Chemicals

Nystatin, pyranine (8-Hydroxypyrene-1,3,6-trisulfonic acid trisodium salt) and the ionophores valinomycin, and FCCP (carbonyl cyanide 4-(trifluoromethoxy) phenylhydrazone) were obtained from Sigma Aldrich Química (Sintra, Portugal). 1-palmitoyl-2-oleoyl-*sn*-glycerol-3-phosphocholine (POPC), DPPC and ESM were purchased from Avanti Polar Lipids (Alabaster, AL, USA). *trans*-Parinaric acid (*t*-PnA) was from Santa Cruz Biotechnology (Santa Cruz, CA, USA). All organic solvents used were Spectronorm grade from VWR (Lisboa, Portugal).

Nys was stored at - 20°C shielded from light. Nys concentration in stock solutions was determined spectroscopically using molar absorption coefficient $\varepsilon = 6.3 \times 10^4\ M^{-1}cm^{-1}$ in ethanol at 304 nm. The lipids and their stock solutions in chloroform were also kept at - 20°C. Their concentrations were determined by phosphate quantification [28]. The fluorescent probe stock solution was stored at - 20°C and its concentration was determined using a molar absorption coefficient of $8.9 \times 10^4\ M^{-1}cm^{-1}$ at 300 nm for *t*-PnA in ethanol [29].

Liposome preparation

Large unilamellar vesicles (LUV) of POPC/DPPC and POPC/ESM binary mixtures were prepared by extrusion of multilamellar vesicle suspensions through polycarbonate Nuclepore Track Etch Membrane filters with 100 nm pore size from Whatman® (GE Healthcare, Little Chalfont, UK) as previously described[30]. The suspension medium was HEPES buffer (Hepes 10 mM pH 7.4, with 150 mM NaCl) and the final lipid concentration was 3 mM, except for partition experiments, where the total lipid concentration was varied. The probe-to-lipid ratio used for *t*-PnA was 1/500. In the preparation of supported lipid bilayers (SLB) for AFM studies, extrusion was performed using polycarbonate filters with 400 nm pore size. Lipid suspensions were stored overnight protected from light.

Absorption and fluorescence measurements

Absorption spectroscopy was carried out with a V-530 or V-560 spectrophotometer from Jasco (Easton, MD, USA). Absorption spectra were corrected for turbidity by subtracting an appropriate blank sample.

Fluorescence measurements were carried out with a Spex Fluorolog 3-22 spectrofluorimeter from Horiba Jobin-Yvon (Edison, NJ, USA) in right angle geometry. Unless otherwise stated, samples and fluorimeter were thermostated at 25°C. Steady-state fluorescence measurements were carried out under constant stirring with excitation (λ_{ex}) and emission (λ_{em})

View Article Online
DOI: 10.1039/C7CP05353C

wavelengths set to 304 nm and 404 nm for Nys and *t*-PnA. Bandwidths were typically 4 nm in both excitation and emission. Fluorescence anisotropy was determined as previously described [23]. Nys activity experiments were performed in a microplate reader (Spectramax Gemini EM), using 405 nm and 450 nm as the excitation wavelengths and 510 nm as emission wavelength. The experiments were performed at 25°C.

Time-resolved fluorescence measurements were carried out by the time-correlated single-photon timing technique[31] using a FluoroHub Controller and a TBX detector with 50 ps time resolution from Horiba Jobin-Yvon. NanoLED sources N-320 and N-370 (with a band pass filter UGI-370) from Horiba Jobin-Yvon (Edison, NJ, USA) were used for excitation of Nys or *t*-PnA, respectively. The number of counts in the peak channel was 20000 using *ca*. 1000 channels per curve over a time window of 50, 100 or 200 ns depending on sample. A suspension of diluted colloidal silica (Ludox®, Sigma) was used to determine the instrument response function.

Data analysis was carried out using a non-linear, least-squares iterative re-convolution method based on the Marquardt algorithm and using the TRFA software (Minsk, Belarus) for lifetime data analysis as previously described [23].

Nystatin partitioning experiments

The dependence of Nys partition coefficient on the lipid composition of the liposomes was assessed from the increase in its steady-state fluorescence intensity upon partitioning into POPC/DPPC or POPC/ESM bilayers. Nys (5 μM) was added to the mixtures (total ethanol was always kept below 1% v/v to prevent liposome destabilization due to the organic solvent[32]) and samples were kept overnight at room temperature and shielded from light for Nys incorporation and equilibration. Samples and fluorimeter were thermostated at 25°C for at least 2 h before the measurements.

Nys water/membrane partition coefficient K_p was determined per Eq. 1:

$$\Delta I = \frac{\Delta I_{max} K_P [L]}{[W] + K_P [L]} \quad \text{(Eq. 1)}$$ [33]

where, $\Delta I = I - I_0$ is the difference between the steady state fluorescence intensity of the antifungal measured in the presence (I) and in the absence (I_0) of lipid vesicles; $\Delta I_{max} = I_\infty - I_0$ is the maximum value of this difference, with I_∞ the limiting value of I corresponding to complete membrane partitioning of Nys, [L] is the total lipid concentration in the suspension, K_p is the mole-fraction partition coefficient of the antifungal between the lipid and aqueous phases and [W] is the molar concentration of water at the assay temperature.

Nystatin activity assays

Nys effect on the potassium permeability of lipid vesicles was determined by H^+/K^+ exchange assays across the membrane bilayer [34]. The methodology for pyranine encapsulation in LUVs (100 nm) was performed as previously described (Carreira et al., 2017 [34]). Briefly, LUVs with 10 mM total lipid concentration were prepared using *K*-buffer (20 mM Hepes; 100 mM K2SO4, pH 7.4) containing 0.5 mM pyranine. The non-encapsulated fluorescent probe was separated from the vesicle suspension using a Sephadex G-25 gel filtration column (dilution factor 1:2) equilibrated with *K*-buffer. LUVs suspension was incubated 10 minutes with FCCP (FCCP:lipid ratio 1:470) to allow for free equilibration of H^+ ions and then a transmembrane K^+ gradient of 3.3:1 $[K^+]_{in}$:$[K^+]_{out}$ was obtained by liposome dilution in an osmotically balanced potassium free buffer (20 mM Hepes-KOH, pH 7.4; 230 mM sucrose; 3 mM NaN_3). After *ca*. 8 minutes, Nys (5 to 15 μM final concentration) was added to the lipid suspension. Nys pore formation causes a K^+ efflux that leads to the acidification of intra-vesicular medium. Consequently, there is a shift in the fluorescence excitation maximum of the entrapped pH sensitive probe pyranine from 450 nm to 405 nm. Accordingly, a decrease in the ratio of the fluorescence intensities measured at 510 nm after excitation at 450 nm and 405 nm is observed upon Nys-induced membrane permeabilization. The fluorescence measurements were performed at 24°C, in a microplate reader (Spectramax Gemini EM). The auto-mix option of the microplate reader was selected to mix the samples 5 seconds before the first read and 3 seconds between reads. Total dissipation of the K^+ gradient was achieved after the addition of the ionophore valinomycin to the liposomes (*ca*. 50 min). Total recovery of the initial fluorescence intensity ratio was achieved by adding Triton X-100 at 0.1% (v/v).

Atomic Force Microscopy Studies

AFM imaging in liquid was performed as described previously[32], using a Multimode Nanoscope IIIa Microscope from Digital Instruments/Veeco. Topographic images were taken with a scan rate of *ca.* 2 Hz in tapping mode. The chosen area of the SLB was scanned repeatedly for at least 30 min to assure that tip scanning had no detectable effects on the height, shape and domain organization of the lipid bilayer.

The glass block holding the cantilever was washed several times with water and ethanol before each experiment. The cantilevers used were made of silicon nitride (SNL, *ca.* 0.35 N/m of spring constant from Bruker) with a resonance frequency in liquid of *ca*. 9 kHz.

The SLB were prepared using LUVs of *ca*. 400 nm diameter and adding 5 mM of calcium chloride to facilitate vesicle fusion and adhesion to freshly cleaved mica. 150μL of LUVs were incubated on the mica surface at 60°C for 1 h to further assist fusion and assembly of a planar SLB and then re-equilibrated at room temperature. Finally, excess lipid was washed several times with buffer [30].

Successive additions of Nys (1.5 μL of Nys containing 0.05 and 0.11 nmol and corresponding to *ca.* 7 and 15 μM in the LUV fluorescence assays) or ethanol (1.5 μL to determine the effect of solvent addition to the SLB corresponding to 1.3 and 2.6% (v/v)) were performed and the same region was imaged between each addition for at least 1 h or until no further alterations of the SLB were observed.

The images presented are representative of each sample. Height or thickness differences were obtained as explained elsewhere [32]. The values are the mean ± standard deviation of

View Article Online
DOI: 10.1039/C7CP05353C

Table 1 Mole-fraction partition coefficients, K_p, of Nys towards POPC/ESM or POPC/DPPC mixtures containing different lipid composition.

Lipid	X_{lipid}	X_{gel}	K_p (x10^4)	S.D. (n≥3)
POPC	100.0	0	1.40 [38]	(± 0.20)
ESM	0.20	0.00	0.72	(± 0.30)
	0.50	0.21	1.96	(± 0.08)
	0.58	0.52	3.03	(± 0.14)
	0.70	0.98	2.32	(± 1.77)
	0.80	1.00	2.21	(± 0.67)
	1.00	1.00	6.51	(± 3.80)
DPPC	0.20	0.00	1.00	(± 0.14)
	0.50	0.23	0.81	(± 0.38)
	0.58	0.38	1.69	(± 0.19)
	0.90	0.98	2.46	(± 0.12)
	1.00	1.00	1.27	(± 0.14)

at least 15 measurements. Images were analyzed regarding gel domain size, area fraction (which can be converted into mole fraction) using the software ImageJ (v1.47 from National Institutes of Health, USA).

Results

Nystatin membrane partitioning behavior

To quantitatively evaluate the effects of Nys in the membrane it is necessary to know the values of the partition coefficient of Nys towards the membrane and relate them with the lipid composition and properties of the vesicles, particularly the extent of gel phase present in each mixture.

The fraction of gel phase is obtained from the respective phase diagrams. Thus, for POPC/DPPC, the fraction of gel phase was taken from previously published phase diagrams [35,36] (see also Figure S1). The phase diagram obtained for POPC/ESM mixtures (Figure S1) is similar to POPC/palmitoyl-SM phase diagram[37], and was used to determine the gel phase fraction of POPC/ESM mixtures. To determine the partition coefficient, K_p, of Nys towards the membrane, the emission intensity of Nys was measured for the different lipid mixtures and plotted as a function of lipid concentration, as exemplified in Figure S2 for POPC/ESM mixtures containing 20 mol% and 50 mol% of ESM. The values of K_p retrieved for each lipid molar fraction and corresponding gel phase fraction (calculated from the respective phase diagram presented in Figure S1) are summarized in Table 1.

For DPPC-containing mixtures, K_p apparently increased due to the mere presence of the saturated phospholipid. However, the increase became more significant for DPPC mole fractions higher than 50%, i.e., in the presence of substantial fractions of DPPC-enriched gel phase. In ESM-containing mixtures however, K_p increase was more pronounced and occurred only in the presence of the gel phase. The results show a strong interaction between the antifungal and the model membranes used, which are dependent both on the lipid type and properties of the gel phase. Nys partition is stronger towards SL-rich membranes, particularly in the presence of the SM-enriched gel phase.

Nys incorporation within the membrane

To further understand the mode of action underlying Nys-membrane interaction, time-resolved measurements of Nys intrinsic fluorescence were carried out (Figure 1).

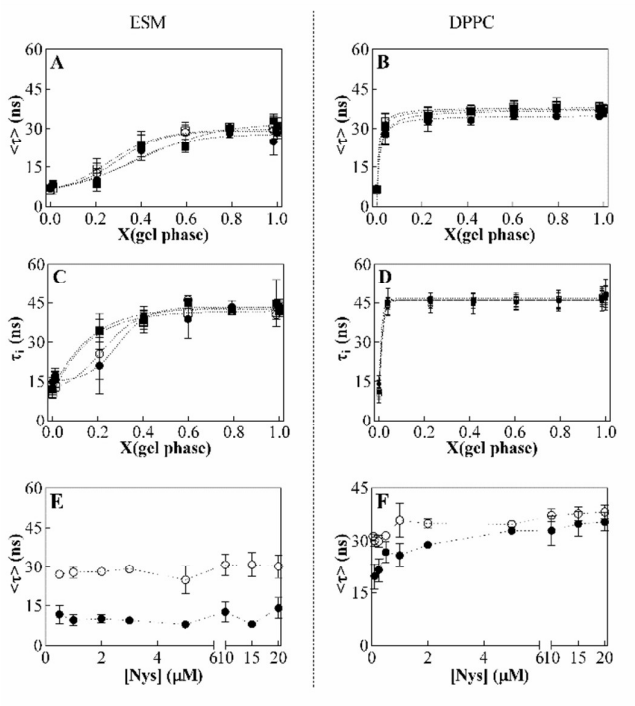

Figure 1: Influence of gel phase fraction on Nys photophysical properties.

(A,B,E,F) Nys mean fluorescence lifetime (<τ>) and ***(C,D)*** long-lifetime component of Nys fluorescence intensity decay (τ_i) measured on LUVs containing **(left - *A,C,E*)** POPC/ESM and **(right - *B,D,F*)** POPC/DPPC as a function of fraction of ***(A-D)*** gel phase present and ***(E,F)*** Nys concentration. ***(A-D)*** The studied Nys concentrations were 5 (●), 10 (○), 15 (■) and 20 μM (□). ***(E,F)*** The effect of Nys concentration was studied for ca. 20% (●) and ca. 98% (○) of gel phase, corresponding to ***(E)*** 50 mol% and 70 mol% of SM or ***(F)*** 50 mol% and 90 mol% of DPPC. Results are the average ± SD of at least 3 independent experiments. The dotted lines correspond to a non-linear fit of the data to a sigmoid growth curve ***(A,C*** and ***D)*** or hyperbola ***(B)***, or connecting lines ***(E,F)***.

Nys displays a complex fluorescence intensity decay characterized by multiple exponentials [38,39]. The mean fluorescence lifetime (<τ>) is therefore a value that represents the ensemble average behavior of Nys molecules. Accordingly, an increase in Nys mean fluorescence lifetime (Figure 1.A,C) might be due to increase in the packing of the membrane [40] as the gel phase fraction increases (Figure 1.B,C), or due to formation of Nys oligomers [38].

Nys long-lived species (<τ> > 20 ns) were detected only in the presence of the gel phase. In fluid phase membranes, only short-lived Nys species (<τ> ~ 5 to 7 ns) were observed regardless of DPPC or ESM presence. In contrast, the increase

View Article Online
DOI: 10.1039/C7CP05353C

in Nys mean fluorescence lifetime was dependent on the type of lipid forming the gel phase. Within DPPC-containing membranes, a very small fraction of DPPC-gel (4% of gel phase/ 40 mol% of DPPC) was sufficient to promote a steep increase in Nys mean fluorescence lifetime and formation of the long-lived Nys species. In ESM-containing membranes however, a larger amount of ESM-enriched gel phase (20% of gel phase / 50 mol% of ESM) resulted in only a slight increase in Nys mean fluorescence lifetime. Furthermore, maximal mean fluorescence lifetime values were lower for ESM-containing membranes (*ca.* 32 ns) compared to DPPC-containing membranes (*ca.* 38 ns), suggesting that Nys molecules are more strongly stabilized upon incorporation into a DPPC-enriched gel phase.

To further analyze the organization of the antifungal in the different membrane environments, the longer lifetime component of Nys intensity decay (τ_i) was plotted as a function of gel phase fraction (Figure 1.C-D).

For POPC/DPPC mixtures (Figure 1.D) a clear boundary between a state of short-lived (for $\tau_i \sim 10$ ns) and long-lived ($\tau_i \geq 30$ ns) fluorescent Nys species is observed, respectively, in the absence and presence of the gel phase. In ESM-containing membranes (Figure 1.C), an increase in the long lifetime component towards values typical of long-lived species is observed upon increasing the fraction of ESM-enriched gel phase. Moreover, the appearance of a long lifetime component of Nys fluorescence intensity decay is dependent on Nys concentration in mixtures containing lower gel phase fraction (20% of gel phase corresponding to 50 mol% of ESM).

To determine if Nys concentration was the limiting factor in the formation of long-lived species, the mean fluorescence lifetime was measured for very low Nys concentrations (Figure 1.E,F). In a DPPC-enriched gel phase (Figure 1.F), the amount of Nys present is a limiting factor dictating the formation of long-lived Nys species. Moreover, an increase in DPPC-gel phase fraction decreased the concentration of Nys required to observe long-lived species. In contrast, in ESM-enriched membranes (Figure 1.E) the fraction of the gel phase is the main limiting factor determining the formation of long-lived species, as suggested by the unvarying fluorescence lifetime of Nys along the range of antifungal concentrations studied. Instead, increase in Nys mean fluorescence lifetime was only observed upon increasing ESM-gel phase fraction (Figure 1.A) or for the lowest concentration of Nys and ESM-gel phase.

Altogether the results suggest that different mechanisms govern the interaction of Nys with bilayers of different lipid composition.

Nystatin-induced membrane leakage

The appearance of long-lived Nys species has been previously associated to the formation of Nys aggregates in the membrane that would correspond to Nys pores [39], which are in turn thought to be responsible for the cytotoxicity and antifungal activity of Nys[41]. However, the increase in the fluorescence lifetime of the antifungal might also be due to incorporation of Nys into the gel phase. This would stabilize the tetraene moiety in its excited state, thus contributing to an increase in the fluorescence lifetime of Nys, analogously to what has been previously described for other tetraene fluorescent molecules [29]. To evaluate Nys ability to form pores in sterol-free membranes well-established permeability assays were performed[20]. As described in the experimental section, the dissipation of a potassium gradient through K^+/H^+ exchange was followed using a liposome encapsulated pH-sensitive probe pyranine. Figure 2.A,B,E,F shows the variation of the internal pH of the vesicles over time after adding either 5 or 15 μM Nys to lipid mixtures of different composition (POPC/ESM with 20, 50 and 70 mol% of ESM and POPC/DPPC with 20, 50 and 90 mol% of DPPC corresponding to 0, 20 and 98% of gel phase in both systems). The data are expressed as the ratio of Pyranine fluorescence intensity obtained upon excitation at the wavelength corresponding to the maximum when Pyranine is at neutral (450 nm) and when is at acidic (405 nm) pH. To further compare Nys effects on membrane permeability, the percentage of gradient dissipation was calculated for different time points (Figure 2.C,D,G,H) [39].

The results showed that both the initial membrane permeabilization and extent of gradient dissipation were significantly slower/lower in membranes lacking gel-fluid phase separation. The presence of gel phase enhanced Nys effects on membrane permeability regardless of the lipid involved in gel phase formation. However, both the initial membrane permeabilization and extent of gradient dissipation were strongly dependent on membrane lipid composition.

Indeed, in the first minute after Nys addition, the membrane permeabilization was faster and increased in the presence of ESM-containing membranes compared to DPPC-containing membranes. It should further be noticed that both these parameters depended not only on the lipid constituents of the membrane, but also on the fraction of the gel phase present. Increasing the fraction of DPPC gel phase led to a slight decrease in the initial membrane permeabilization, but an overall increase in the extent of gradient dissipation. This is likely due to a slower partition of the Nys molecules into the membrane because of its tight packing and absence of membrane packing defects. Note that a similar effect was observed in control experiments where only valinomycin was added to the mixtures (Supplementary Figure S3.C,D): in mixtures containing 100% DPPC gel phase the rate and extent of gradient dissipation caused by valinomycin was slower/lower, but probably did not reach the equilibrium value within the timeframe of the experiments. This observation further supports the hypothesis that partition and/or incorporation of molecules within a DPPC rigid gel phase is slower.

In membranes containing ESM gel phase, the initial membrane permeabilization and extent of gradient dissipation was dependent both on the fraction of gel phase, and on Nys concentration. In contrast to observed for DPPC membranes, the extent of gradient dissipation was higher immediately upon addition of Nys to the membranes, and decreased over time. These results suggest that Nys might induce other effects in the vesicles, that could allow exposure of some Pyranine

View Article Online
DOI: 10.1039/C7CP05353C

molecules to the external aqueous environment and, therefore, to a neutral pH, leading to a partial recovery of a higher 450 nm / 405 nm intensity ratio. Alternatively, Nys might induce membrane lateral and transversal reorganization, enhancing the intrinsic membrane permeability or rendering it permeable to other ions such as chloride. Under these conditions, the H^+ ions would cross the membrane until pH equilibrium is reached. Independently of the mechanism leading to pH gradient dissipation, it can be concluded that Nys is the key player, since similar effects are not observed in control experiments where

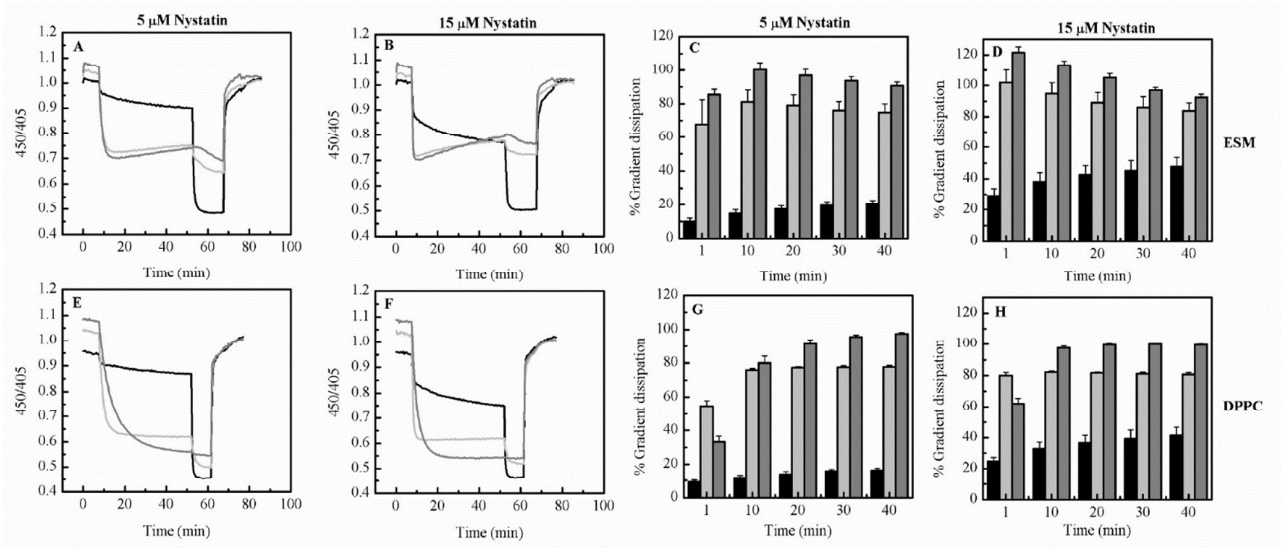

Figure 2: Nystatin-induced membrane permeabilization.

(A,B,E,F) The fluorescence intensity of entrapped pyranine after dilution in K^+ free buffer was evaluated overtime through ratiometric measurements of pyranine excited at 450 and 405 nm (450/405). Nys was added to the samples at ap. 8 minutes and Valinomycin was added at ap. 50 minutes to ***(A,B)*** POPC/ESM and ***(E,F)*** POPC/DPPC mixtures. ***(A,E)*** 5 μM and ***(B,F)*** 15 μM of Nys were added to POPC containing ***(A,B)*** 20, 50 and 70 mol% (black, light grey and dark grey, respectively) of ESM and ***(E,F)*** 20, 50 and 90 mol% (black, light grey and dark grey, respectively) of DPPC. After *ca*. 60 ***(E,F)*** and ***(A,B)*** 70 minutes, triton X100 (0.1% (v/v)) was added to samples to recover the initial fluorescence intensity ratio. These experiments were repeated at least three independent times and the values are median representative curves of those experiments. ***(C,D,G,H)*** The percentage of gradient dissipation was calculated at different time points after the addition of ***(C,G)*** 5 and ***(D,H)*** 15 μM Nys to POPC containing ***(C,D)*** 20, 50 and 70 mol% (black, light grey and dark grey bars, respectively) of ESM and ***(G,H)*** 20, 50 and 90 mol% (black, light grey and dark grey bars, respectively) of DPPC. Data are the mean ± standard deviation of at least 3 independent experiments. In all these experiments 20 and 50 mol% of ESM or DPPC correspond to 0 and 20% of gel phase, respectively. Vesicles with 98% of gel phase are represented by 70 mol% of ESM and 90 mol% DPPC.

only valinomycin is added. In contrast, adding valinomycin to the vesicles causes dissipation of the K^+ gradient and acidification of the inner vesicular space through H^+ influx (Figure S3.A,B).

Overall, the results show that kinetics and extent of Nys pore formation occur via different mechanisms that are not restricted to the formation of well-organized membrane pores, and depend on lipid composition and presence of gel-fluid phase separation.

Nys effect on membrane lipid organization and properties

Data obtained from Nys-permeability assays suggest that, depending on membrane lipid composition and biophysical properties, changes in membrane permeability might be due to either the formation of Nys active species (pores) or membrane destabilization. Therefore, to further clarify the mechanism underlying Nys interaction with the bilayer, particularly to evaluate the effects of Nys on the biophysical properties and lateral organization of the lipids, AFM studies were performed using binary POPC/ESM and POPC/DPPC supported bilayers on mica with gel/fluid phase coexistence. The effective Nys:lipid ratio in the supported bilayer can be estimated from the partition coefficients in Table 1 and the lipid concentrations in these systems[42]. Under our experimental conditions, this ratio is in the order of 1:1000, so that any changes observed can be solely attributed to alterations in lipid phases properties. The compact nature of the gel phase causes an increase in lipid bilayer thickness which translates into height difference of approximately 0.5 to 2.0 nm between the gel and fluid phases[43].

Analysis of POPC/DPPC (Figure 3) and POPC/ESM (Figure 4 and Figure 5) mixtures showed the coexistence of fluid and gel phases with the expected fraction of lipid phases in correlation to lipid composition, in accordance with the phase diagrams for each lipid mixture (Figure S1.B,C) [35,36,43]. As reported in previous studies [44], the gel domains were *ca*. 1.2 and 2 nm thicker than the fluid[32], for DPPC and ESM respectively.

The effects of AFM repetitive scanning and solvent were tested by comparing domain morphology and topography before and after continued imaging of the samples for over 1 h and by the addition of Nys solvent, ethanol (data not shown). While the former did not lead to any detectable changes, each ethanol addition caused a slight increase in height gap between the gel domains and the fluid from 1.2 to 1.6 nm and 1.0 to 1.2 nm for POPC/ESM and POPC/DPPC SLBs, respectively. All these observations are similar to those previously described for SLBs

View Article Online
DOI: 10.1039/C7CP05353C
Phys. Chem. Chem. Phys. ARTICLE

composed of phospholipid binary mixtures displaying gel/fluid phase coexistence [32].

Nys addition to POPC/DPPC 50:50 (Figure 3) mixtures caused a significant two-dimensional swelling of the gel phase by 50% and 10% for successive additions (from *ca.* 30% to 45% and 55%) (Figure 3.C). The last addition of Nys caused a small decrease in the thickness difference between gel and fluid (Figure 3.C). Nys effect was noticed solely on the gel phase occurring immediately after the addition and remaining stable for over 1 h of incubation.

Nys fluorescence lifetime (Figure 1) and induced membrane permeabilization (Figure 2) showed a strong dependency on ESM membrane content and ESM phase fraction. Therefore, AFM studies were performed for SLBs containing two different

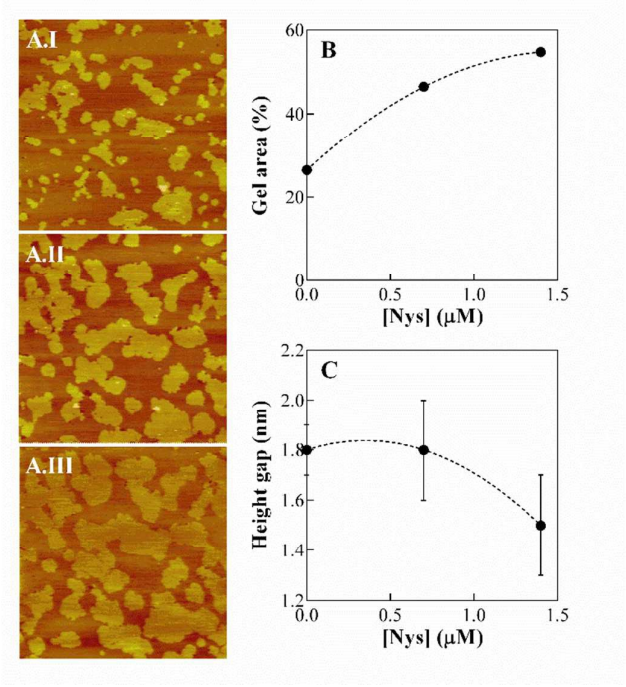

Figure 3: Nys effect on POPC/DPPC membrane domain morphology.
(*A*) AFM images for SLBs of POPC/DPPC 50:50 **(*A.I*)** before adding Nys and after the **(*A.II*)** first and **(*A.III*)** second addition of Nys, corresponding to final Nys concentrations of 0.7 and 1.4 μM, respectively. 20 x 20 μm^2; z = 10 nm. **(*B*)** Percentage of ordered phase area and **(*C*)** height gap between the fluid and gel domains for POPC/DPPC before and after each Nys addition.

ESM mole fractions, one where the maximum value of Nys fluorescence lifetime had been attained, and another where the fluorescence lifetime is in between the maximum and the value in fluid, i.e., POPC/ESM 30:70 and 50:50, respectively (Figure 1).

For the highest ESM fraction (70 mol%, Figure 4), Nys only had any noticeable effect after the second addition (1.4 μM), which led to a modest (two-dimensional) swelling of the gel domains.

After a third addition of Nys (2.1 μM), an 'expanded gel' phase, which protruded from the original gel domains was observed. This new phase was thinner than the original gel by *ca*. 0.7 nm and occupied as much as approximately 10% of the bilayer area (Figure 4.A.IV, B, C). Any observed changes occurred within the first minutes after Nys addition, and remained stable for over 1 h.

For the composition POPC/ESM 50:50 (Figure 5), which contains ca. 20 % gel, a gradual expansion of the ESM gel phase into the 'expanded gel phase' was observed from the first addition of Nys (0.7 μM). Just as observed for the ESM 70 mol% membrane, the 'expanded gel phase' appeared at the edge of the gel domains. The rounder domains of increased area (by *ca*. 35-40 %) and reduced height-gap (by *ca*. 0.8 nm) appeared over a period of ca. 2 h as depicted in the time series images of Figure 5.A. Further incubation with the same Nys concentration resulted in complete destabilization of the original gel domains. Considering that the thickness of the expanded gel, as well as its localization, lays between the ones of the gel and the liquid-disordered (l_d) phases, this new phase may resemble a liquid-ordered (l_o) phase. In fact, AFM phase imaging of this system, which contains information regarding the material properties (namely viscoelasticity), shows that the expanded gel displays unique features that differ both from the gel and the l_d phases (Fig. S4).

For a membrane containing 50 mol% of ESM and presenting ca. 20% of ESM-enriched gel phase, mean fluorescence lifetime measurements performed under equilibrium conditions (Figure 1) and real-time gradient dissipation measurements showed that Nys incorporation/aggregation and gradient dissipation occurred to a small extent and only for the highest concentration of Nys. Real-time AFM studies showed that gel phase fraction changes not only with Nys concentration but also with time. In order to ascertain if the formation of Nys long-lived species were also time-dependent, particularly in POPC/ESM mixtures, Nys fluorescence lifetime was measured overtime in mixtures containing 20% gel phase fraction (Figure 5.E). The results showed that Nys molecules present a long mean fluorescence lifetime and elevated long lifetime component for up to 15 min after interaction with the measured after overnight incubation (Figure 1.A,C,E). The disappearance of the long-lived species coincides with the disappearance of the ordered gel-phase and formation of the membranes. Within 30 min, the values decrease to those 'expanded-gel phase' as observed by AFM, Moreover, the disappearance of the long lived Nys species was faster upon increasing the Nys to lipid molar ratio, in agreement with AFM data (data not shown).

AFM studies further confirmed that Nys interaction with the bilayer depends both on membrane composition and biophysical properties.

Discussion

The observation of highly ordered, ergosterol-free and sphingolipid-enriched gel microdomains in the membrane of Nys sensitive yeast [23] raised the question of how mandatory is the presence of sterols for the organism sensitivity to polyene macrolides. We hypothesized that antifungal activity on

View Article Online
DOI: 10.1039/C7CP05353C

membranes can be governed by the presence of tightly-packed sterol-independent gel domains. Synthetic biology approaches were used to develop a model mimicking these domains.

A low T_m phospholipid (POPC) common in eukaryotic biological membranes, and a high T_m lipid, either a mammalian sphingolipid (ESM) or a saturated glycerophospholipid (DPPC), were used to compare the effect of both gel phase properties and lipid composition on Nys-membrane interactions.

Nys partition was higher for ESM compared to DPPC-enriched membranes and specific Nys-lipid interactions may regulate Nys membrane partitioning. Although both high T_m lipids are structurally similar, their small differences affect H-bonding patterns at the head-water interface and the acyl chain packing of the gel phase [37,45]. Consequently, the packing defects created at the interface between the gel and the fluid phases in the DPPC vs. the ESM-containing membranes appear to be different, as also suggested from the different shapes of the domains observed by AFM, which might determine the differences in interaction of the antifungal molecules with the bilayer. Indeed, Nys partition and interaction with the membrane was enhanced in mixtures displaying gel-fluid phase separation. The interface between different phases is characterized by packing defects, which act as preferential sites for the incorporation of external molecules [46,47]. Previous studies of Nys partitioning towards lipid membranes have shown that Nys partitioning increased in the presence of a gel phase as opposed to a fluid phase [40] and that sterol type or content do not strongly affect partition in the absence of a phase separation [20].

The results obtained in the present study showed that Nys interaction with the lipid bilayer is modulated both by the type of membrane lipid components and the biophysical properties of the membrane itself [18,48].

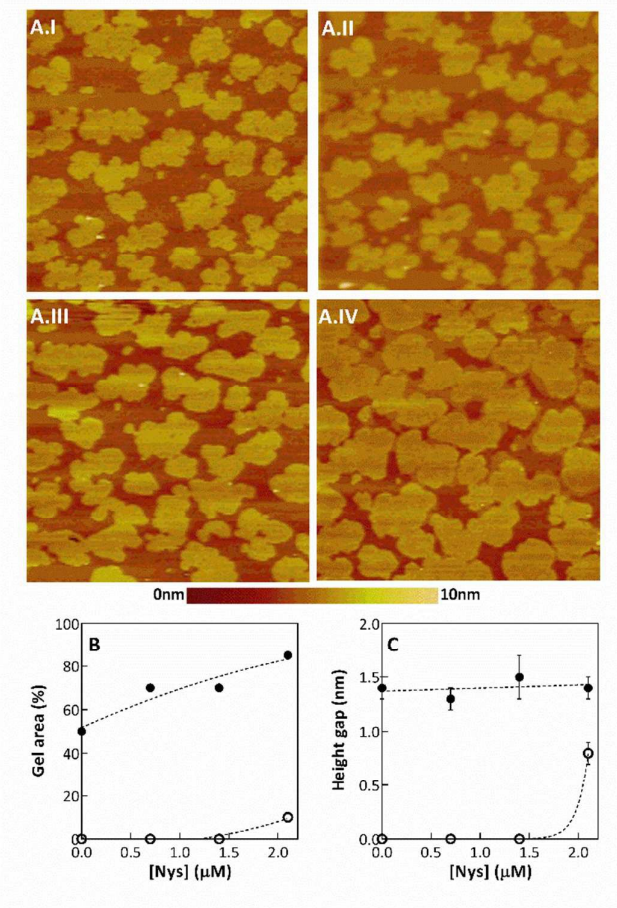

Figure 4: Nys effect on POPC/ESM 30:70 membrane biophysical properties.

(*A*) AFM images of POPC/ESM 30:70 SLBs before adding Nys **(A.I)** and after successive additions of 0.7 μM of Nys **(AII-AIV)**. 20 x 20 μm^2; z = 10 nm. **(*B*)** Percentage of gel phase area and **(*C*)** height gap between the fluid phase and the gel phase (●, full circles) or between the fluid phase and the expanded gel phase (○, open circles) for each Nys addition.

Nys interaction with DPPC-containing membranes

In DPPC-containing membranes, a small fraction (*ca*. 4%) of gel phase was enough to enhance the adsorption and concomitant incorporation of Nys molecules within the bilayer. This was observed by the increase in the partition coefficients of Nys, which reflects an increase in the number of molecules interacting with the hydrophobic lipid bilayer, and by the increase of its fluorescence lifetime values, which indicates an increased molecular rigidity [23,29]. Longer Nys fluorescence lifetimes are evidence for incorporation of Nys into the bilayer and can result from the formation of Nys aggregates into barrel-like oligomers, with the chromophores closely packed in a parallel conformation [49]. Indeed, upon interacting with the membrane, Nys induces a two-dimensional swelling of the DPPC-enriched gel phase, suggesting a direct interaction of the antifungal molecules with this phase. The tight packing of the lipids within this ordered phase confers stability to Nys tetraene fluorescent moiety, decreasing its non-radiative decay rate, and therefore elongating its fluorescence lifetime. The lack of membrane thinning and the presence of K^+ leakage, suggests that the pores might consist of membrane spanning structures likely consisting of two half pores [50]. Moreover, domain morphology was also unaffected suggesting that Nys-induced gel expansion is likely governed by Nys inclusion into the gel-phase. These results agree with recent studies showing that depending on Nys/lipid chain hydrophobic match, Nys can induce gel domain formation [47,51,52]. In summary, in DPPC-containing membranes, the increase in Nys fluorescence lifetime is likely to reflect both situations, *i.e.*, increased molecular rigidity due to incorporation into an ordered lipid phase and formation of Nys aggregates.

The formation of Nys active species, presumably barrel-like oligomers, able to dissipate a transmembrane ion gradient is dependent on the presence of DPPC-gel phase fraction and, for shorter incubation times, on Nys concentration. Indeed, in the absence of gel phase, an increase in Nys concentration results in a faster initial membrane permeabilization and larger extent of gradient dissipation. However, these parameters became only marginally dependent on Nys concentration in the presence of DPPC gel phase. This suggests that Nys ability to permeabilize the membrane depends strongly on the

View Article Online
DOI: 10.1039/C7CP05353C

properties of the membrane, but also on the number of Nys molecules interacting with the membrane, particularly when gel phase is not present.

Nys interaction with ESM-containing membranes

As observed for DPPC-containing membranes, the fluorescence lifetime of Nys is only weakly dependent on total Nys concentration, and thus this is not the only factor governing the formation of long-lived Nys species. Indeed, long-lived species are present only when membranes contain a large fraction of ESM-gel phase or very low Nys concentration, suggesting that a threshold of Nys/fraction of ESM-enriched gel phase ratio is crucial for the formation of those long-lived species. This is likely related to the ability of Nys to destabilize ESM-enriched gel phase, as shown by AFM imaging. In the case of ESM, the gel phase is strongly dependent on the H-bonding network established between the ESM molecules. Insertion of Nys molecules within this gel phase likely disturbs the regularity of

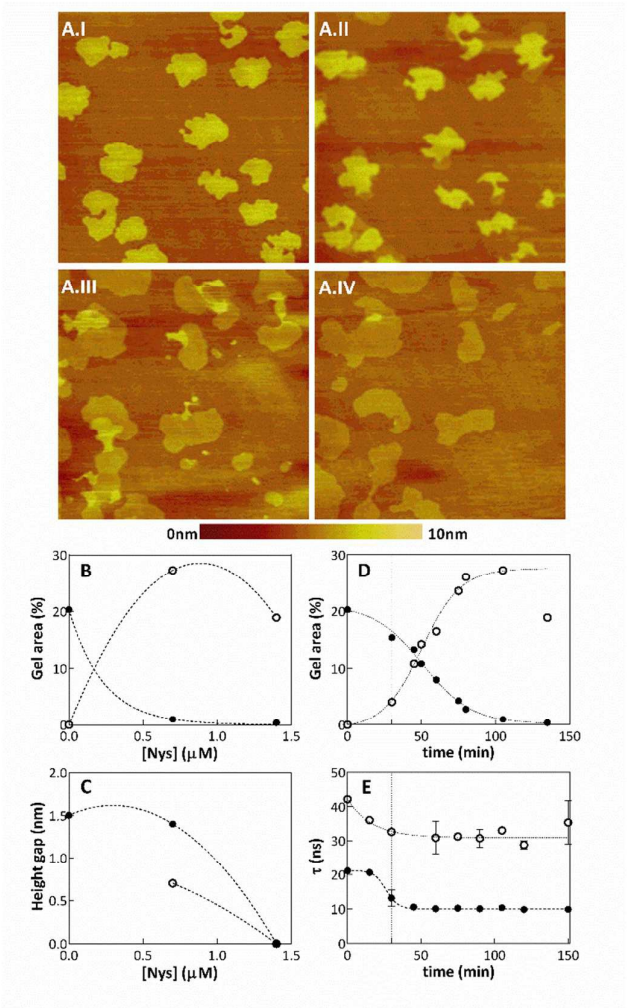

Figure 5: Nys effect on POPC/ESM 50:50 membrane biophysical properties. **(*A*)** AFM images of POPC/ESM 50:50 SLBs before adding Nys **(*A.I*)** and 35min **(*A.II*)**, 1h10 **(*A.III*)** and 1h45 **(*A.IV*)** after the addition of 0.7 μM Nys. 20x20μm^2 images depicting the height of the sample from 0 to 10 nm by a color gradient (darker to lighter color, respectively). **(*B*)** Percentage of area and **(*C*)** height gap between the fluid phase and the gel phase (●) or expanded gel phase (○) before and after successive additions of 0.7 μM Nys. **(*D*)** Variation of the percentage of area of gel domains (●) and expanded gel domains (○) obtained from AFM imaging and **(*E*)** variation of Nys mean fluorescence lifetime (<τ>, ●) and long-lifetime component (τ_l, ○) over time upon addition of Nys to LUVs at equivalent Nys:lipid ratio.

this network with concomitant formation of a less packed, more expanded ESM/Nys ordered-like phase. Accordingly, formation of an expanded gel phase with unique structural and material properties and disappearance of the original thicker ESM- enriched phase is observed upon increasing Nys/ESM-gel fraction ratio. This change of membrane organization and properties occurs concomitantly with the disappearance of Nys long-lived species, showing that formation of these long-lived species mostly reflects a stabilization of the Nys tetraene moiety by the ordered phase, rather than the presence of Nys oligomers. This suggests that Nys mechanism of permeabilization in ESM-containing membranes is most likely associated with Nys-induced membrane reorganization and abolishment of ESM gel domains. Moreover, the destabilization of the ordered phase is likely caused by Nys self-association into active pores, that cause the fast and extensive membrane permeabilization observed prior to ESM-gel phase abolishment. Thus, there seems to be an interesting type of self-terminating mechanism of the formation of organized Nys-oligomers in ESM-containing membranes. A similar effect of membrane thinning upon transmembrane pore formation was proposed for antimicrobial peptides that was ascribed to a favorable decrease in the elastic energy of the membrane [51].

It should be further stressed, that the observed reduction in membrane thickness compared to the original gel phase and expansion of the 'destabilized gel phase' is also consistent with an increase in the hydration of the bilayer and an overall disordering of the phase, and might indicate the creation of a region with interfacial characteristics [53] that might enhance permeation of H^+ and possibly other ions through the membrane, and dissipation of the pH gradient initially caused upon Nys addition. A similar effect is observed by other membrane destabilizing agents, such as small alcohols, where the phenomenon would correspond to an increased spacing between phospholipid headgroups that is filled with the organic molecule, inducing imperfections in lipid packing [32,54]. Both membrane thinning and Nys-insertion at the domain boundary are indicative of a mechanism of pore formation dependent upon the reduction of interfacial energy [55,56]. Moreover, the overtime destabilization of the ESM-enriched gel domains may also indicate ESM depletion from the domain due to specific Nys-ESM interactions in a lipid diffusion limited process. The proposed hypotheses are not mutually exclusive and may provide insight into a broader understanding of the

View Article Online
DOI: 10.1039/C7CP05353C

molecular mechanisms behind Nys pore formation and selectivity.

Importantly, these results show that Nys strongly influences membrane organization of SM-enriched areas, highlighting that studies that take advantage of this molecule to sequester Chol from lipid-raft like domains should be regarded with caution, since Nys effects on the membrane will not be limited to its interaction with Chol.

Conclusions and Biological Implications

The present work shows that the formation of Nys active species depends both on the type of lipid and the presence of ordered gel domains inasmuch that: i) only moderate membrane permeabilization is observed in fluid membranes; ii) Nys interaction leading to pore formation occurred at the gel/fluid domain boundaries and iii) gel domain properties and composition affected Nys membrane stabilization and Nys-induced membrane permeabilization.

Our results suggest that Nys-membrane interactions are dependent on the presence of the specific membrane packing defects that characterize each gel/fluid system and Nys/lipid chain mismatch, which increase Nys insertion into the membrane and promote a stabilization of the molecule within the bilayer allowing for stable pore formation. The DPPC-enriched gel phase could successfully and extensively incorporate and stabilize the Nys molecules and lead to Nys oligomerization into rigid active pores. In contrast, formation of these oligomers disturbed the tight packing properties of a sphingolipid-enriched gel phase, probably by interfering with the H-bond network established between sphingolipid molecules. Under these conditions, Nys active species are only formed when the number of Nys molecules within the membrane is high enough to perturb the structure and organization of ESM-enriched gel domains.

Overall, this work pinpoints that Nys-induced membrane permeabilization is related to its effects on membrane properties and organization, and this depends on membrane lipid composition and, thus, on the ability of Nys to interact differently with membranes displaying distinct membrane biophysical properties. This work further suggests that although Erg might remain one of the key factors in explaining Nys antifungal activity, other membrane properties need to be considered when addressing Nys molecular mode of action and cytotoxicity. A more comprehensive knowledge of Nys mode of action is pivotal for the development of lipid-based nanoparticles that can efficiently incorporate significant amounts of the antifungal and target lipid domains specific to fungal membranes, such as the SL-enriched sterol-free gel domains identified in yeast [23].

Acknowledgements

This work was supported by Fundação para a Ciência e Tecnologia (FCT), I. P., Portugal (grant numbers PTDC/BBB-BQB/6071/2014, PTDC/BBB-BQB/3719/2014, UID/MULTI/00612/2013), FCT PhD grant SFRH/BD/88194/2012 to A.C.C. and Investigador FCT grants IF/ 00437/2014 to LCS, IF/00317/2012 to RFA and IF/00808/2013 to AV.

Notes and references

1 A. Chakrabarti, 2011, **15**, 97–103.
2 S. B. Zotchev, *Curr. Med. Chem.*, 2003, **10**, 211–23.
3 J. Bolard, *Biochim. Biophys. Acta*, 1986, **864**, 257–304.
4 H. A. Gallis, R. H. Drew and W. W. Pickard, *Rev. Infect. Dis.*, 1990, **12**, 308–29.
5 W. I. Gruszecki, M. Gagos and P. Kernen, *FEBS Lett.*, 2002, **524**, 92–6.
6 H. Ishibashi, A. J. Moorhouse and J. Nabekura, in *Patch Clamp Techniques*, Springer Japan, 2012, pp. 71–83.
7 J. K. Volkman, *Appl. Microbiol. Biotechnol.*, 2003, **60**, 495–506.
8 C. M. Richman-Boytas and L. W. Parks, *Microbios*, 1989, **59**, 101–111.
9 T. E. Andreoli, *Ann. N. Y. Acad. Sci.*, 1974, **235**, 448–468.
10 B. de Kruijff, W. J. Gerritsen, A. Oerlemans, R. A. Demel and L. L. M. van Deenen, *Biochim. Biophys. Acta*, 1974, **339**, 30–43.
11 P. van Hoogevest and B. de Kruijff, *Biochim. Biophys. Acta*, 1978, **511**, 397–407.
12 K. S. Récamier, a Hernández-Gómez, J. González-Damián and I. Ortega-Blake, *J. Membr. Biol.*, 2010, **237**, 31–40.
13 K. Hac-Wydro and P. Dynarowicz-Latka, *Biophys. Chem.*, 2006, **123**, 154–61.
14 K. Hąc-Wydro, J. Kapusta, A. Jagoda, P. Wydro and P. Dynarowicz-Łątka, *Chem. Phys. Lipids*, 2007, **150**, 125–135.
15 L. Kristanc, S. Svetina and G. Gomiščck, *Biochim. Biophys. Acta - Biomembr.*, 2012, **1818**, 636–644.
16 M. E. Kleinberg and A. Finkelstein, *J. Membr. Biol.*, 1984, **80**, 257–269.
17 J. Bolard, P. Legrand, F. Heitz and B. Cybulska, *Biochemistry*, 1991, **30**, 5707–15.
18 L. Kristanc, B. Božič and G. Gomiščck, *Biochim. Biophys. Acta - Biomembr.*, 2014, **1838**, 2635–2645.
19 A. Marty and A. Finkelstein, *J. Gen. Physiol.*, 1975, **65**, 515–26.
20 L. Silva, A. Coutinho, A. Fedorov and M. Prieto, *Biochim. Biophys. Acta*, 2006, **1758**, 452–9.
21 J. González-Damián and I. Ortega-Blake, *J. Membr. Biol.*, 2010, **237**, 41–9.
22 C.-C. HsuChen and D. S. Feingold, *Biochem. Biophys. Res. Commun.*, 1973, **51**, 972–978.
23 F. Aresta-Branco, A. M. Cordeiro, H. S. Marinho, L. Cyrne, F. Antunes and R. F. M. De Almeida, *J. Biol. Chem.*, 2011, **286**, 5043–5054.
24 A. Leber, P. Fischer, R. Schneiter, S. D. Kohlwein and G. Daum, *FEBS Lett.*, 1997, **411**, 211–214.
25 R. F. M. de Almeida and E. Joly, *Front. Plant Sci.*, 2014, **5**, 72.
26 S. N. Pinto, E. L. Laviad, J. Stiban, S. L. Kelly, A. H. Merrill, M. Prieto, A. H. Futerman and L. C. Silva, *J. Lipid Res.*, 2014, **55**, 53–61.

View Article Online
DOI: 10.1039/C7CP05353C

27 M. L. Kraft, *Mol. Biol. Cell*, 2013, **24**, 2765–8.
28 G. Rouser, S. Fleischer and A. Yamamoto, *Lipids*, 1970, **5**, 494–496.
29 L. A. Sklar, B. S. Hudson, M. Petersen, J. Diamond and R. D. Simoni, *Biochemistry*, 1977, **16**, 819–828.
30 J. T. Marquês, A. M. Cordeiro, A. S. Viana, A. Herrmann, H. S. Marinho and R. F. M. De Almeida, *Langmuir*, 2015, **31**, 9410–9421.
31 J. R. Lakowicz, *Principles of Fluorescence Spectroscopy*, Springer Science+Business Media, LLC, New York, 3rd edn., 2006.
32 J. T. Marquês, A. S. Viana and R. F. M. De Almeida, *Biochim. Biophys. Acta*, 2011, **1808**, 405–14.
33 S. H. White, W. C. Wimley, A. S. Ladokhin and K. Hristova, *Methods Enzymol.*, 1998, **295**, 62–87.
34 A. C. Carreira, R. F. M. De Almeida and L. C. Silva, *Sci. Rep.*, 2017, **7**, 1–16.
35 P. J. Davis, K. P. Coolbear and K. M. Keough, *Can. J. Biochem.*, 1980, **58**, 851–858.
36 W. Curatolo, B. Sears and L. J. Neuringer, *Biochim. Biophys. Acta*, 1985, **817**, 261–70.
37 R. F. M. de Almeida, A. Fedorov and M. Prieto, *Biophys. J.*, 2003, **85**, 2406–16.
38 A. Coutinho and M. Prieto, *Biophys. J.*, 2003, **84**, 3061–78.
39 A. Coutinho, L. Silva, A. Fedorov and M. Prieto, *Biophys. J.*, 2004, **87**, 3264–76.
40 A. Coutinho and M. Prieto, *Biophys. J.*, 1995, **69**, 2541–57.
41 Š. Z. Jokhadar, B. Božič, L. Kristanc and G. Gomišček, *PLoS One*, 2016, **11**, e0165098.
42 J. T. Marquês, A. S. Viana and R. F. M. de Almeida, *Langmuir*, 2014, **30**, 12627–12637.
43 A. Berquand, N. Fa, Y. F. Dufrêne and M. P. Mingeot-Leclercq, *Pharm. Res.*, 2005, **22**, 465–475.
44 P. R. Maulik and G. G. Shipley, *Biophys. J.*, 1996, **70**, 2256–65.
45 S. L. Veatch and S. L. Keller, *Phys. Rev. Lett.*, 2005, **94**, 148101.
46 E. G. Chulkov, S. S. Efimova, L. V Schagina and O. S. Ostroumova, *Chem. Phys. Lipids*, 2014, **183**, 204–7.
47 A. Koukalová, Š. Pokorná, R. Fišer, V. Kopecký, J. Humpolíčková, J. Černý and M. Hof, *Biochim. Biophys. Acta - Biomembr.*, 2015, **1848**, 444–452.
48 C. S. Helrich, J. a Schmucker and D. J. Woodbury, *Biophys. J.*, 2006, **91**, 1116–27.
49 M. A. R. B. Castanho, A. Coutinho, M. J. E. Prieto and M. J. E. Prietos, *J. Biol. Chem.*, 1992, **2**, 204–209.
50 F. Foglia, M. J. Lawrence, B. Demeė, G. Fragneto and D. Barlow, *Sci. Rep.*, 2012, **2**, 778.
51 F.-Y. Chen, M.-T. Lee and H. W. Huang, *Biophys. J.*, 2003, **84**, 3751–3758.
52 E. G. Chulkov, S. S. Efimova, L. V. Schagina and O. S. Ostroumova, *Chem. Phys. Lipids*, 2014, **183**, 204–207.
53 M. Eeman and M. Deleu, *Biotechnol. Agron. Soc. Environ.*, 2010, **14**, 719–736.
54 E. I. Goksu, J. M. Vanegas, C. D. Blanchette, W.-C. Lin and M. L. Longo, *Biochim. Biophys. Acta*, 2009, **1788**, 254–66.
55 P. I. Kuzmin, S. A. Akimov, Y. A. Chizmadzhev, J. Zimmerberg and F. S. Cohen, *Biophys. J.*, 2005, **88**, 1120–1133.
56 B. E. Cohen, *J. Membr. Biol.*, 2010, **238**, 1–20.